Experimental study of a powerful energy flow effect on materials in PF-I000 installation

Michal Borowiecki,
Paola De Chiara,
Aleksandr V. Dubrovsky,
Elena V. Dyomina,
Vladimir A. Gribkov,
Lev I. Ivanov,
Sergej A. Maslyaev,
Franco Mezzetti,
Ryszard Miklaszewski,
Valerij N. Pimenov,
Linda Pizzo,
Marek Scholz,
Adam Szydlowski,
Yulo E. Ugaste,
Igor V. Volobuev

Abstract The report describes some of the results obtained in an experimental study of the impact of a powerful plasma stream and a fast ion beam generated in a PF-1000 device on different materials perspective for the use in radiation loaded parts of pulsed plasma installations. Investigations were done during and after the interaction processes. It is shown that in case of irradiation of samples only by high power flux density plasma streams the effect of detachment still preserved. At the same time a low power flux density high-energy ion beam plays an important role in the process of saturation of the irradiated material by hydrogen.

Key words dense plasma focus • irradiation • plasma jet • shock wave • test specimen

M. Borowiecki, R. Miklaszewski, M. Scholz
Institute of Plasma Physics and Laser Microfusion,
Hery Str. 23, 00-908 Warsaw, Poland

A. V. Dubrovsky✉, V. A. Gribkov, I. V. Volobuev
P.N. Lebedev Physical Institute, Russian Academy of Sciences,
Leninsky pr. 53, 117924 Moscow, Russia
Tel.: +7 095/ 1326651, e-mail: adubrov@mail.ru

E. V. Dyomina, L. I. Ivanov, S. A. Maslyaev, V. N. Pimenov
A.A. Baikov Institute of Metallurgy and Material Science,
Russian Academy of Sciences,
Leninsky pr. 49, 117334 Moscow, Russia

P. De Chiara, F. Mezzetti, L. Pizzo
Dipartimento di Fisica dell´ Universitá di Ferrara
and Instituto Nazionale di Fisica della Materia (INFM),
Via Paradiso 12, I-44100 Ferrara, Italy

A. Szydlowski
The Andrzej Soltan Institute for Nuclear Studies,
05-400 Swierk by Warsaw, Poland

Y. E. Ugaste
Pedagogical University of Tallinn,
Narva Road 25, 10120 Tallinn, Estonia

Introduction

This work presents first results of experimental investigations of plasma-surface interaction, which follow the purpose of an INCO-COPERNICUS Contract, forming our International team. It has been done on the Mather-type 1 MJ Plasma Focus device PF-1000 [11] and it continues our previous works made on a plasma device of the same type [4, 5, 8]. The difference between the two experiments is that in the previous case we used another electrode geometry (Filippov type) and a lower energy stored in the bank (about 60 kJ). Also specimens irradiated in these two cases and working gases were different, whilst in both experiments those samples have been placed at the cathode side of the device.

But to have the possibility to compare our previous results with the present ones obtained at a much higher level of energy stored in the capacitors, we have positioned our samples in this case at a distant of about 10 times further from the source than in the previous experiments.

Experimental methods

Tested materials

Materials selected for this study, shape and dimensions of specimens, as well as modes of their manufacturing are presented in Table 1. The choice in favor of these materials has been determined by the fact that austenitic

Table 1. Specimens tested in PF-1000 experiment.

Material	Chemical content of test material (mass %)	Specimen form	Specimen dimensions mm	Specimen manufacturing method
Steel 25Cr12Mn20W	0.25-C, 12-Cr, 20-Mn, 1-W	Plate	15 × 15	Fusion, Rolling
Steel 10Cr12Mn20W	0.1-C, 12-Cr, 20-Mn, 1-W	Plate	15 × 15	Fusion, Rolling
Technical Copper	99.5% Cu	Tablet	∅12	Fusion, Rolling, Cutting, Grinding
Alloy Copper + Nickel	Cu+4% Ni	Tablet	∅10	Fusion, Cutting, Grinding
Alloy Copper + Gallium	Cu+10% Ga	Tablet	∅10	Fusion, Cutting, Grinding
Vanadium Alumothermal	99.4% V	Tablet	∅12	Fusion, Rolling, Grinding
Tungsten Monocrystal		Tablet	∅15	Guiding decrystallization, El.-erosive cutting, Grinding
Carbon high-purity		Tablet	∅12.5	Cutting, Grinding

chromo-manganese steels, pure vanadium, tungsten, carbon, copper, as well as alloys on their basis, are the materials of substantial stability and resistance to high radiative or thermal effects [1, 6]. Besides, the materials are corrosion stable and have high mechanical and high technological characteristics [3, 12]. Moreover, it is important to stress that many of them meet the demands necessary to fulfil for its use in pulsed high current devices. Thus, it is possible to consider these materials as perspective ones for utilization in high-energy load units of modern installations to be exposed by any pulse powerful impact of different nature, mainly in a sphere of pulsed high-current electronics. At the same time, some of the tested materials (e.g. tungsten and carbon) are considered also as most perspective ones for Tokamak divertor and its first wall [7, 9].

Test steel samples have been smelted as the ingots and then have been rolled to 0.1 cm thick. Other material specimens were made by means of cutting from blank rods.

Experimental installation

The sample irradiation experiment has been carried out on the dense plasma focus (DPF) installation PF-1000 (Poland) [11]. In this work the DPF device was operated with the energy store of 580 kJ. Pure hydrogen was used as a working gas with an initial pressure of 200 Pa. Scheme of the experiment is presented in Fig. 1. It should be stressed that this set of experiments was at the same time a first step in the optimization procedure for this biggest in the world device of this type. A lot of improvement should be done here. Its present mode of operation as well as its electrode dimensions and power flux densities reached are as yet very preliminary ones.

A special construction made it possible to place a single specimen, or a couple of them, into the irradiation zone, while not disturbing the vacuum conditions in the DPF chamber. The sample holder has been fixed on the tip of a long metallic arm of 49 mm in diameter inserted through the center of the PF chamber from a cathode side along the chamber axis. In order to protect a test sample from a discharge current due to short circuit, a final segment of the arm, 10 cm long, has been made from a plastic insulator. The distance from the source of radiation – "plasma focus" – to the test specimens could be varied from zero up to 175 cm. We have chosen 60 cm as the right distance for the first series of an irradiation experiment. The total discharge current, as well as a hard X-ray radiation pulse, was registered in each DPF shot (Fig. 2). The value of the discharge current typical for PF-1000 being operated at noted conditions

and with a relatively long internal electrode (anode, length flat solid upper lid) is about 1.5 MA.

Preliminary series of DPF shots (so-called conditioning of the chamber) were undertaken in order to put the DPF device into maximal flux of fast ions generation mode of operation attainable with the above mentioned construction. At this optimization procedure, we have considered a value of initial gas pressure as a general parameter, which determines different modes of the DPF device operation. "Roentgen Gamma dosimeter 27040" was used to measure a dose of the hard X-ray radiation in each DPF shot. As a result of the preliminary series of shots, an initial hydrogen pressure of 200 Pa has been chosen as the optimum for the main stage of the experiment, because the hard X-ray radiation dose maximum corresponds to this value. We took it as a principal factor in these experiments because the necessary (yet not the only) condition for an efficient ion beam generation in DPF is a well-developed electron acceleration process.

Several steel test specimens have been irradiated during the preliminary series of shots (the above conditioning procedure). But our basic quantity of test samples was irradiated during the main experimental stage and in the regime when 3 successive DPF shots have been used for irradiation of each test specimen. The total number of irradiated samples was 26.

The fast ion flux (time integrated) acting on a test sample was registered by means of a CR-39 track detector [10], which was located close to the sample holder. A fast streak
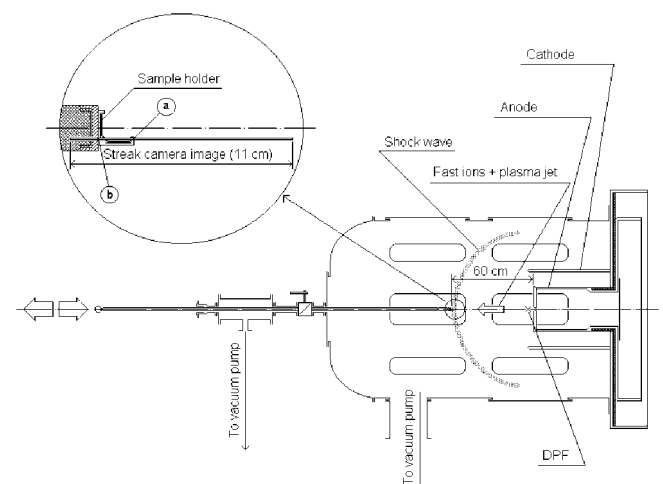

Fig. 1. The scheme of PF-1000 irradiation experiment.

camera (see Fig. 1) investigated the dynamics of a hot plasma jet in the vicinity of specimen during its flying up to a specimen and under the interaction of it with the sample.

Methods of analytical investigation of samples

After irradiation, the samples were investigated by optical and scanning electron microscopy. X-ray structural and X-ray spectral analyses were used to study the surfaces of both irradiated and reference (not irradiated) samples. Thickness of a layer, which was evaporated during the interaction of a high-energy pulse with a specimen, was determined by precise weighing it before and after the action with proper calculations.

Experimental results

Irradiation parameters, strictly speaking, the surface of each irradiated specimen placed at a cathode side of the device was subjected to at least 5 irradiation factors as a result of each DPF shot [2]. Being enumerated according to the moment of their impact onto a test sample, they are as follows (in the described experiment and with a distance of 60 cm between the anode and specimen).

1. Hard X-ray and soft X-ray radiation (just at the moment of DPF formation – 2 ns time-of-flight (TOF)).
2. Fast hydrogen ion beams (several hundred ns TOF after X-ray pulse).
3. Shock waves (6 μs TOF after X-ray pulse).
4. Plasma jets (6–8 μs TOF after X-ray pulse).
5. A cloud of relatively cold substance, spreading from the DPF anode, which consists mainly of anode material (copper) ions (more than 10 μs TOF after X-ray pulse).

We have paid attention generally to factors #2, #3, and #4 as the most powerful ones. However, sometimes we noted also an effect of factor #5 on the specimen surface realized as obvious copper film spots covering sample surfaces.

According to our experience, and as it is also known from the literature, the pulse duration of the DPF fast ion beam as well as the time of hard X-ray generation process is of the same order of magnitude. As it is seen in Fig. 2, this time is equal approximately to 200 ns for the PF-1000 device. Powerful ion beam emits along Z-axis in the direction of the DPF cathode, where our test specimen is placed. This beam is subjected to a certain time-of-flight expansion on its way to test sample (up to a few microseconds). We have estimated the energy spectrum (time integrated), as well as the fluence of the ion beam by means of a CR-39 track detector [10]. A magnified picture of the detector surface after proper development process is presented in Fig. 3. Our method makes it possible to register the authentic flux of fast ions within the energy range 70 keV $\leq E_i \leq$ 10 MeV. It is known from the literature that the fast hydrogen ion beam generated in DPF has the energy spectrum not exceeding the upper limit of this region. It is known that maximal DPF fast ions intensity is related to the energy range of 70 keV $\leq E_i \leq$ 130 keV. This is supported by our analysis of the tracks. Thus, we consider fixed by track detector ions as the ones in full belonging to this spectral range. The main result of the track detector method used is that the total number of fast hydrogen ions per square centimeter, which had an impact on the test specimen surface per each single DPF shot, is $(0.6–2.0) \times 10^5$ cm^{-2}. It is important to note here that the indicated relatively low value corresponds just to the described non full-scale experiment. As it was mentioned above, our next step in optimization of PF-1000 is to change electrode dimensions and shape to have the possibility to increase the installation energy store and convert the device to the ion beam production mode of operation. Also the distance from a zone of the ion beam generation to the irradiated sample is to be decreased.

Fortunately, it was possible for us in the present experiments to investigate our plasma cumulative stream (jet) with time resolution and to calculate its dynamics numerically. 2-Dimensional MHD code of Z-pinch discharge (version 30.11.99) by Prof. V.V. Vikhrev [13] was applied in conformity with our geometry as well as with all other operational parameters of the PF-1000 device. According to the results of the calculation, the plasma jet flies up to the test specimen at a speed of 10^7 cm/sec. In the region close to the specimen surface the jet plasma density is $n = (2–3) \times 10^{17}$ cm^{-3}, plasma temperature T = 10–20 eV at the time, which proceeds to the beginning of plasma-surface interaction process. When plasma jet irradiates normally oriented "test sample" surface, it stops and compresses. Because of con-
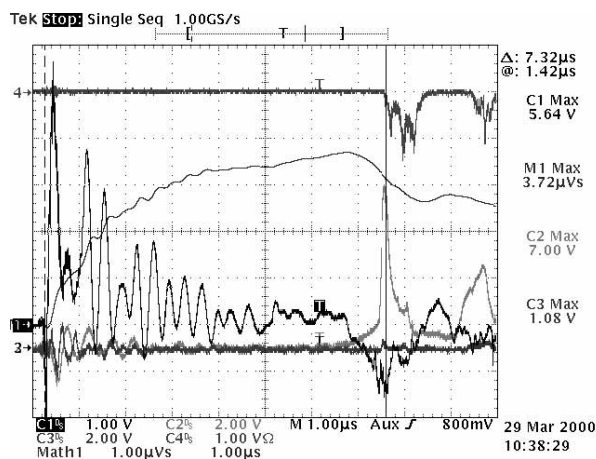

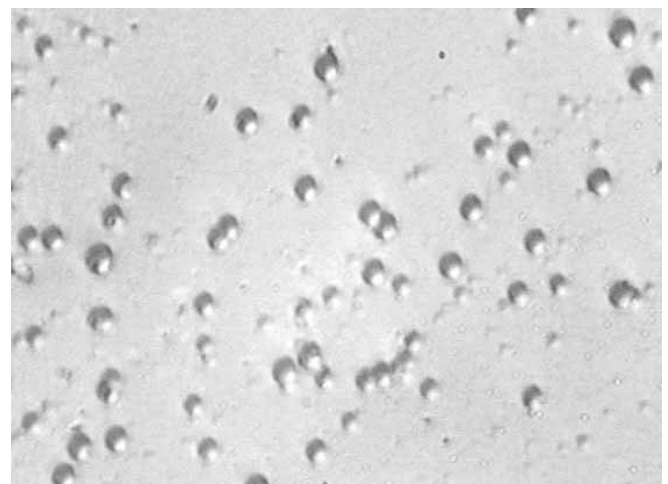Fig. 2. Oscilloscope traces of DPF current and hard X-ray pulse.

Fig. 3. Photo of fast ions tracks obtained by means of CR-39 detector.

version of the directed motion of plasma particles into chaotic thermal movement of them, the plasma density increases up to $n = 1.5\times10^{18}$ cm^{-3}, whereas the plasma temperature rises up to $T = 250$ eV. The interaction process lasts about 1.5–2.0 μs according to the calculations.

It should be taken into account that in these calculations we ignored all processes connected with the "internal target problem", such as thermal conduction into the target, evaporation of the target, etc. So, we may use these results as the initial conditions for the whole multi-staged dynamical problem which looks as follows:

• formation and transportation of a jet from a pinch to the target (fast process),
• interaction of a jet with a target (fast process),
• heating and evaporation/ionization of it, accompanied by a compression of the target (fast),
• formation of a cloud in front of the target ("detachment process" – medium),
• relaxation of the compressed target and subsequent material release from its surface (so-called "unloading wave" – slow process),
• diffusion of the absorbed gas from the implanted layer (very slow process).

But main characteristics of the jet plasma near the target will not be too much influenced by the 'internal target problem' if the power flux density of the jet on the sample surface is high enough (above 10^8 W/cm^2). In this case the jet will produce fast target evaporation, ionization and plasma heating up to temperatures of the order of those obtained in the calculation. We shall now compare our calculations with the experimental results obtained.

The experimental study of plasma jet dynamics in the vicinity of irradiated test sample, carried out by means of fast streak camera, shows that some bright layer (precursor) foreruns in front of a basic luminous plasma cloud (see Fig. 4). The picture makes it possible to determine a thickness of the layer as $l = 1.96\pm0.05$ cm, and the velocity of a plasma jet as $v = 8.8\pm0.2\times10^6$ cm/sec. It is important to note that during these experiments our streak camera has been positioned at the level about 1.5 cm below the device axis (as it is shown in Fig. 1). Therefore, two points of the sample holder – (a), and (b) – were seen in the streak camera image. Bright luminescence of those points takes place when the plasma jet begins to interact with these parts of the sample holder. One can see that bright points initially appear on the photo about 1.5 cm to the right-hand direction from their real positions (which was determined by geometrical measurements and seen later in time). This fact can be explained by a deflection of the light ray by spherical shock wave (SW). A front of the SW is able to operate as an optical lens, if the plasma density rises on the front of this wave up to the value exceeding $n = 10^{18}$ cm^{-3} (thus its gradient will be large enough). We have made an attempt to present in a sketchy manner a spherical plasma shock wave in Fig. 1. So our evaluation of plasma density as $n \geq 10^{18}$ cm^{-3} certainly fits well to the plasma near the device axis at the moment of arriving a shock wave produced by the jet. Intensive plasma-surface interaction at the points (a) and (b) lasts about 1 μs according to the presented photo, but already after about 0.25 μs the plasma density gradient
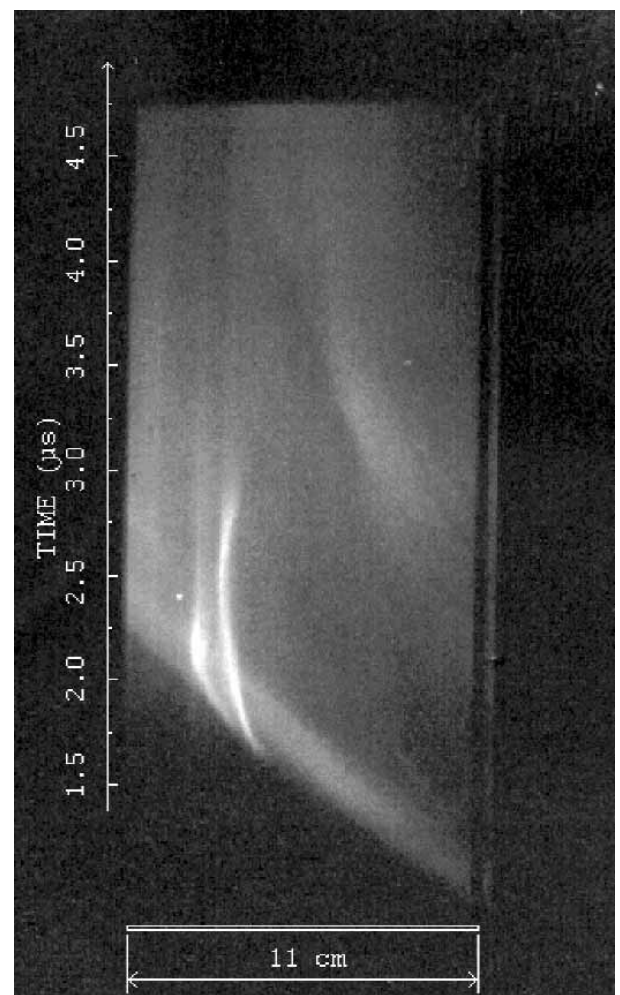

Fig. 4. Photo of streak camera image.

becomes very low and the bright spots come back on its "prescribed" position (no density gradient – no deflection). Also at this moment brightness of those spots becomes higher. These last facts are in favor of thermalization of the jet resulted in a strong evaporation process, which takes place at the sample surface and develops during this time interval. Our estimations of the lower limit for the power flux density on the target gave us a value above 10^9 W/cm^2.

Subsequent analytical investigations made with the samples have shown that for each test specimen its surface state has been changed as a result of the irradiation. Evidently due to the jet/SW impact strongly displayed phenomena of surface melting, evaporation, and sputtering of the components take place. Accurate weighing of specimens before and after the effect of irradiation undoubtedly fixes perceptible loss of mass. For example, being evaluated as loss of thickness under one DPF shot, the shortage of copper as well as based on copper (see Table 1) samples is estimated as 0.5 ± 0.1 μm per shot.

But also there are some features resulting from the interaction of fast ions with the surface (being in the melted state because of the powerful jet action). A specific nature of the surface topography structure of irradiated specimens containing melted drops as well as blistering or/and crater formation phenomena are evident. Two pictures of steel samples surface taken after the irradiation, which have been obtained by means of scanning electron microscopy are pre-
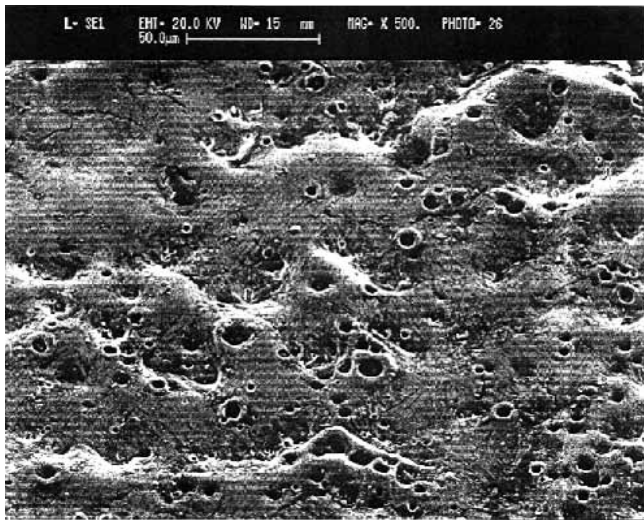
Fig. 5. The surface of 25Cr12Mn20W steel specimen after 3-fold hydrogen plasma pulse irradiation in PF-1000 device. Crater surface structure is evident.
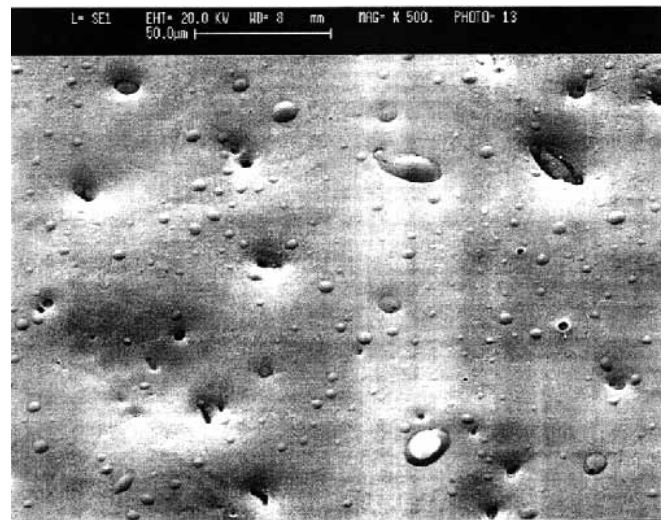

Fig. 6. The surface of 10Cr12Mn20W steel specimen after 8-fold hydrogen plasma pulse irradiation in PF-1000 device. Blistering phenomenon formation is evident.

sented in Figs. 5 and 6 as examples. Basic analytical results relating to the described experimental study will certainly be published later. Now we just note multifarious surface change because of the radiation action that we can observe on test specimens depends mostly on sample material. However, the presented pictures take the opportunity to attract attention to the fact that the craters as well as blisters density at the sample surface, evaluated on the photo, is equal in the order of magnitude to the fast ions of surface density.

Discussion

In our previous study, produced at the very well optimized installation "TULIP" [4, 5, 8] (energy storage $E = 60$ kJ) we considered that our test specimens were affected by the irradiation of two types. The first one is an ion beam, and the second one is a plasma jet. We had there a short distance between pinch and samples (5 cm). Taking into account a later moment of fast ion beam formation, compared with the one for a jet and different TOF of plasma jet and ion beam bunches, we stated that both types of radiation had an affect on the target simultaneously. Analyzing beam and jet divergence as well as dispersion of both bunches (so its pulse duration), we found that power flux density of jet and beam on the target surface was above 10^8 and 10^9 W/cm^2, correspondingly, whereas the energy deposited by both mechanisms was about the same. Owing to the fact that the pulse energy impact on the test sample surface was dual in character, we have observed some specific effects of the interaction [4]. Namely, under these conditions the so-called 'broken implantation' took place with an evident display of plasma screening of the surface ('detachment effect'). At the same time we have found a very unusual effect. The phenomenon was that the concentration of the implanted deuterons was decreased from the bulk of the material closer to the target surface and it became lower with an increase of the number of shots. It was not so clear what could be the reason for such an effect.

In the recent experiments, the fast ion power flux density was not more than about $\sim 10^{-2}$ W/cm^2 which was fixed by

means of track detector at the place, where test specimens were positioned. At the same time the power flux density for the plasma jet was at the same level as it was in our previous experiments (above 10^9 W/cm^2). Thus, in this case the energy impact on the specimen surface is of single nature (the effect of plasma shock wave and plasma jet are simultaneously arriving events). But again here as in the previous case both the fast ion beam and plasma jet act on a target simultaneously.

Some evaluations based on experimental results obtained by means of a streak camera, as well as certain estimations based on the DPF device energy balance or using computer code calculations, e.g. [13] give rise to energy exposure dosage rate density of 10^9–10^{10} W/cm^2 per one shot of PF-1000. However, reliable evaluation of an absorbed dosage should be adopted as W $\geq 10^8$ W/cm^2 as a result of considering the experimental fact of mass loss by test samples after radiation effect due to evaporation. Therefore, the first conclusion, which can be derived here, is that even in the case of an interaction with the target of jet alone, the screening (preservation) of the target surface by evaporated, in the first moment, target material ("the detachment effect") still takes place. But the power flux density of the jet of these low energy ions (several keV) should be above 10^9 W/cm^2.

Registered fast ions flux of too low power density nevertheless evidently takes an important part in surface modification processes. Indeed, examples of the analytic results (Figs. 5 and 6) presented here demonstrate an important role of the fast ions in different surface conversion phenomena. In particular, working here individually in the process of its interaction with a melted surface of a target, each of these fast ions (about 100 keV) produces blisters or even craters. Thus, our second conclusion is that now it is clear that this feature demonstrates a possible mechanism by which the gas can be released from the sample. Indeed having high energy, the fast ions penetrate into melted material down to a relatively high depth, thus producing channels in it. Gas implanted and diffused into the bulk of the target earlier by means of the plasma jet can now be easily released into these channels and ejected later on. In our

previous experiments the power flux density of ion beam was very high and very close to the one of the jets, so the ions interacted with the target collectively. Thus the whole picture was too complicated and difficult for interpretation. It will be interesting to see what happens when optimization of this devise and conversion it into an ion beam generation mode will increases the ion power flux density up to the same value as for the jet.

In any case, the results obtained at the PF-1000 device now allow us to look forward to posterior new results in plasma-surface interaction study.

References

1. Abe F, Garner FA, Kayano H (1994) Effect of carbon on irradiation hardening of reduced-activation 10Cr-30Mn austenitic steels. J Nucl Mater 212–215:760–765
2. Gribkov VA (2000) On possible formulation of problems of a Dense Plasma Focus used in material sciences. Nukleonika 45;3:149–153
3. Ivanov LI, Maslyaev SA, Pimenov VN et al. (1999) The use of liquid metals in porous materials for divertor applications. J Nucl Mater 271–272:405–409
4. Ivanov LI, Pimenov VN, Demina EV et al. (2000) Interaction of high temperature deuterium plasma streams with condensed materials in Dense Plasma Focus device. In: 14th Int Conf Plasma Surface Interactions in Controlled Fusion Devices. Rosenheim, Germany, May 22–26. Program and Book of Abstracts: 3–51
5. Ivanov LI, Pimenov VN, Maslyaev SA et al. (2000) Influence of dense plasma pulses on materials in Plasma Focus device. Nukleonika 45;3:203–207
6. Kiueh RL, Kenik EA (1994) Thermal stability of manganese-stabilized stainless steels. J Nucl Mater 212–215:437–441
7. Krieger K, Roth J (2000) Synergistic effects by simultaneous bombardment of tungsten with hydrogen and carbon. In: 14th Int Conf Plasma Surface Interactions in Controlled Fusion Devices. Rosenheim, Germany, May 22–26. Program and Book of Abstracts: 0–8.3
8. Maslyaev SA, Pimenov VN, Platov YuM et al. (1998) Influence of deuterium plasma pulses generated in plasma focus device on materials for thermonuclear fusion reactor. Perspektivnye Materialy 3:39–46 (in Russian)
9. Ohya K, Kawakami R, Tanabe T et al. (2000) Simulation calculations of mutual contamination between tungsten and carbon and its impact on plasma surface interactions. In: 14th Int Conf Plasma Surface Interactions in Controlled Fusion Devices. Rosenheim, Germany, May 22–26. Program and Book of Abstracts: 0–8.1
10. Sadowski M, Al-Mashhadani EM, Szydlowski A et al. (1994) Investigation on the response of CR-39 and PM-355 track detectors to fast protons in the energy range 0.2–4.5 MeV. Nucl Instrum Meth Phys Res B 86:311–316
11. Scholz M, Miklaszewski R, Gribkov VA, Mezzetti F (2000) PF-1000 device. Nukleonika 45;3:155–158
12. Vertkov AV, Evtichin IE, Lyublinski IE et al. (1993) Mechanical properties of low activation Cr-Mn austenitic steel changes in liquid lithium. J Nucl Mater 203:158–163
13. Vikhrev VV, Ivanov VV, Rozanova GA (1993) 2-Dimensional MHD code of Z-pinch discharge. Nucl Fusion 33;2:311–321